

Modal Optical Modelling of a Test System for Ultra-Low-Noise Transition Edge Sensors for Space Science

Jiajun Chen, Stafford Withington, Christopher N. Thomas, Orlando Quaranta
Quantum Sensors Group, Cavendish Laboratory, JJ Thomson Avenue, Cambridge CB3 0HE
 *Contact: j.chen@mrao.cam.ac.uk, phone +44(0)1223(7)66468

Abstract— For all high-performance detectors, well-understood optical test systems are needed for precise characterisation and calibration. A cryogenic variable temperature blackbody load has been developed to test the optical efficiencies of ultra-low-noise ($\text{NEP} \sim 10^{-19} \text{ W Hz}^{-1/2}$) Transition Edge Sensors for space science. The few-mode, partially coherent illumination conditions of the measurement system are engineered to be precisely the same as those of the telescope. We have used a SPICA/SAFARI-like telescope/detector for demonstration purposes. The essential difference between the test system and an equivalent representation of the telescope's optics is that the telescope has a lens of effective focal length f , but the test system does not. A key part of our analysis is to describe behaviour in terms of the optical modes of the test system, as distinct from the optical modes of the detector under test. In the paper we describe the analysis of the test assembly in terms of signal power, background power and photon noise.

I. INTRODUCTION

A cryogenic optical test system has been developed to measure the optical efficiencies of ultra-low-noise Transition Edge Sensors (TESs). Such detectors are essential for the next generation of cooled-aperture space telescopes and interferometers. The detectors comprise a planar superconducting absorber behind a few-mode far-infrared lightpipe, and operate with NEP's as low as $2 \times 10^{-19} \text{ W Hz}^{-1/2}$ at 70 mK. A variable temperature (4 K to 25 K) black-body load illuminates the detector under test through a sequence of band-defining optical filters, and the throughput is determined by an aperture, which is designed to illuminate the detector with an optically clean beam. We are working on three different frequency ranges, each of which has its own band-defining filters: L-Band 210-110 μm , M-Band 110-60 μm and S-Band 60-34 μm [1].

It can be shown that the modes of an optical system comprising an aperture, a thin lens and an aperture corresponding to the footprint of the detector, are precisely the same as those of an optical system comprising two apertures of the same size that maintain the same physical opening angle, but without the thin lens. The absence of the thin lens does not alter the transformation of blackbody sources. This is because a lens can be seen as a transformation of phase, while

the phases of blackbody field are essentially, at least over distances of greater than a wavelength, random. By avoiding the use of lenses, a very clean partially coherent optical beam can be established. For our tests we adopted the effective focal ratios of the SPICA telescope: 16.5 for L-Band, and 20 for M-Band and S-Band [2]. Thus the test system presents precisely the same partially coherent illumination conditions as the telescope itself.

Fig. 1 shows a schematic representation of the test assembly. A Variable Temperature Load (VTL) is used as blackbody source. The VTL is based on a gold-plated copper disk connected to an outer case by 3 Kevlar strings, which in turn is connected to the cryostat [2]. The low thermal conductance of the Kevlar guarantees thermal decoupling of the blackbody source from the cryostat [3]. The temperature of the VTL is controlled through the use of 3 heating resistors glued on the surface of the disk and monitored by a calibrated thermometer buried inside the disk. Finally the VTL is connected to the 4 K stage of the cryostat through a copper strap, which determines the thermal relaxation time of the load.

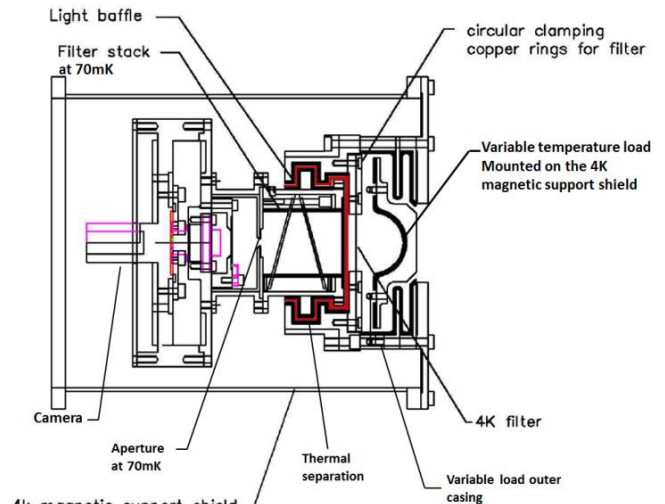


Fig. 1 The mechanical drawing of the main parts of the optical test system

The blackbody radiation generated by the VTL illuminates the detector through a series of band-pass filters (one set for each band) and a circular aperture. The distance between the aperture plane and the detector plane, ℓ , is 10.75 mm. To achieve the same focal ratios for the 3 wavebands of SAFARI, aperture sizes of 651.5 μm for L-Band, and 537.5 μm for M-Band and S-Band are used.

The thermal load generated by the VTL is potentially high and can influence the behaviour of the cryostat, especially at elevated temperatures (e.g. 25 K), therefore the load cannot be connected to the same stage as the detectors and optics (70 mK stage). The outer case of the VTL is connected directly to the magnetic shield (a cylinder that surrounds the entire assembly), which is thermally anchored to the 4 K stage. To further reduce the heat load on the 70 mK stage, an IR filter has been introduced at 4 K. The coaxial symmetry of the system helps guarantee the alignment of the VTL with the optics and lightpipe. This solution leaves an air-gap (shown in red) between the main body of the filter stack and the VTL, thermally decoupling the two. To minimize the possibility of stray light leaking in through this gap, a system of baffles has been introduced. Finally, many of the surfaces were blackened to minimize unwanted reflections that could potentially lead to light leakage and standing waves.

In a previous paper, we presented a comprehensive multi-mode model of the SAFARI/SPICA telescope in the few-mode limit [4]. In this model, the optical system was characterised by a set of natural optical modes. The forms of the modes, and their individual transmission efficiencies, were determined by using classical paraxial optics, based on plane waves, to calculate the Point Spread Function (PSF) as a function of the direction of a point source on the sky. All that is necessary to find the modes is to establish a matrix where each column corresponds to the complex field at the detector plane when a point source is in a particular direction on the sky, and each column corresponds to a sampled raster of directions. This matrix is then factored through Singular Value Decomposition (SVD) to give the modes of the optical system: as distinct from the optical modes of the detector. Note that SVD is needed because the angular distribution of an incoming field on the sky is in a different Hilbert space to that of a spatial field across the image plane. The natural modes of the optical system can then be used together with the modes of the detector to calculate all aspects of behaviour including signal power, photon noise power and stray light.

The same technique has been applied to modelling the behaviour of the test system; in this way we can ensure that measurements carried out with the test system are truly representative of the partially coherent behaviour of the few mode optical system of SAFARI. Calculations of optical throughput, total power loading of the detectors by the source, and photon noise from the source and baffle have been carried out for all wavebands. It has been shown that the modes and modal throughputs of the test system are identical with those of the SAFARI/SPICA optics. The test system provides near identical optical performance to that of the telescope itself.

II. RESULTS

A. Optical Modes of the Test System

The VTL can be modelled as producing the same electromagnetic field at the aperture as a black body in the far-field, but limited spectrally by the filter stack. The diffraction integral can then be used to propagate this field to the plane of the detector. After passing through the aperture, a diffraction integral can be used to calculate the field across the footprint of the input of the detector. For the telescope, the detectors are in the far field of the throughput-defining aperture, whereas for the test system, the detectors are in the near field, thus no simplifications are possible in the analysis. In particular, to calculate the PSF, it is necessary to use full numerical diffraction integrals rather than relying on expressions taken from Fourier optics. The most straightforward method is to numerically calculate the fields on the focal plane. To do so, a matrix \mathbf{T} is populated as a propagator. Each column of \mathbf{T} comprises the sampled Point Spread Function (PSF) across the footprint of a pixel when a plane wave arrives from the blackbody source from some particular direction. Different columns correspond to different directions. The optical modes can then be determined by decomposing the propagator \mathbf{T} using Singular Value Decomposition (SVD): $\mathbf{T} = \sum_n \sigma_n \mathbf{u}_n \mathbf{v}_n^*$, which represents the fact that a set of angular beam patterns, \mathbf{v}_n , maps onto a set of spatial fields in the detector plane, \mathbf{u}_n , in one-to-one correspondence with weighting factor σ_n . The \mathbf{v}_n and \mathbf{u}_n correspond to the natural modes of the optical system, and σ_n^2 corresponds to the optical efficiency of optical mode n at a certain wavelength [4].

B. Power Loading from Source

The blackbody power loading at the detector plane, over the spatial footprint of the input aperture of the detector, can be calculated by integrating the blackbody radiation scaled by the efficiencies, $|\sigma_n|^2$, of the optical modes over the wavebands:

$$P(T) = \sum_n \int_{\nu_{min}}^{\nu_{max}} \eta_n^{opt}(\nu) \frac{2h\nu}{\exp(\frac{h\nu}{kT}) - 1} d\nu, \quad (1)$$

where $\eta_n^{opt}(\nu)$ is the throughput of the optical mode, n , at frequency ν . The total power absorbed by the detector, assuming that a perfect TES absorber is used, can be determined by including the coupling efficiency $\eta_i^{cpl}(\nu)$ between the optical modes and lightpipe modes [4]:

$$P(T) = \sum_i \sum_n \int_{\nu_{min}}^{\nu_{max}} \eta_i^{cpl}(\nu) \eta_n^{opt}(\nu) \frac{2h\nu}{\exp(\frac{h\nu}{kT}) - 1} d\nu, \quad (2)$$

where i denotes the index of the lightpipe modes.

C. Photon Noise from Source

It has been shown that when a power measurement, W , is made on a partially coherent statistically stationary radiation field, the expectation value of the measurement, $E[W]$, can be found in terms of the cross spectral density of the radiation and a tensor that characterises the detector response [5]. The covariance between the fluctuations between the outputs of two pixels, a and b , is $C[W^a, W^b]$. It comprises the noise

associated with classical bunching and the noise due to photon counting: $C[W^a, W^b] = C[W^a, W^b]_c + C[W^a, W^b]_q$ [6]. The first term corresponds to classical noise, and the second term to the quantum noise, with

$$C[W^a, W^b]_c = \frac{1}{\tau} \int_{\nu_{min}}^{\nu_{max}} \text{Tr}\{K^a K^b\} \left[\frac{h\nu}{\exp(\frac{h\nu}{kT}) - 1} \right]^2 d\nu, \quad (3)$$

and

$$C[W^a, W^b]_q = \frac{\delta^{ab}}{\tau} \int_{\nu_{min}}^{\nu_{max}} \text{Tr}\{K^a\} \frac{(h\nu)^2}{\exp(\frac{h\nu}{kT}) - 1} d\nu, \quad (4)$$

where τ is the integration time, and K are matrices that characterise the optical behaviour of the system, e.g. the optical throughputs of the optical modes, and the coupling efficiencies between the optical modes and the waveguide modes. Only classical noise can result in correlations between the outputs of two different pixels. By setting $a=b$ we get the fluctuation noise in the output of a single pixel.

D. Power Loading from Baffle

The temperature of the throughput-defining aperture is 70 mK in the test system. It is crucial to understand how much power from the baffle is seen by the detector. As it is concerned that if loading and noise from baffle will dwarf signal of interest. A simplified calculation of baffle loading and noise has been carried out under the following assumptions: (i) the baffle is a continuous sheet with uniform temperature T ; (ii) the detector is a perfect absorber with area A ; (iii) the detector is sensitive to frequencies ranging from the cut-off frequency of the waveguide to infinity, as there are no band-defining filters between the baffle and the detector. Then the upper-limit to the power loading from the baffle is given by

$$P(T) = \int_{\nu_c}^{\infty} \frac{A\Omega}{\lambda^2} \frac{h\nu}{\exp(\frac{h\nu}{kT}) - 1} d\nu, \quad (5)$$

where Ω is taken to be 2π steradians, as the detector only sees power in the forward direction. Usually this loading can be considered insignificant if the temperature of the baffle is sufficiently low.

III. RESULTS

The above scheme provides an elegant numerical formalism for modelling the performance of the optical test system. Summarising results are presented to illustrate the effectiveness of the method.

A. Optical Modes

Fig. 2 shows the optical modes of the test system using the detector footprint of SAFARI L-Band at the central wavelength, $160 \mu\text{m}$. The intensity beam patterns (top) map onto the intensity focal plane modes (bottom) in one-to-one correspondence. The first, second and fourth optical modes are shown left to right, and the second and third modes are degenerate with their spatial forms rotated by 90 degrees. By comparing the optical modes of the test system with those of the equivalent telescope, it has been shown that the optical modes and their individual throughputs are the same. Fig. 3

shows the associated modal throughputs. The sum of the modal throughputs is 0.289, which corresponds to the usual definition of overall throughput. Indeed, for the telescope, the sum of the spectral throughputs is also 0.290.

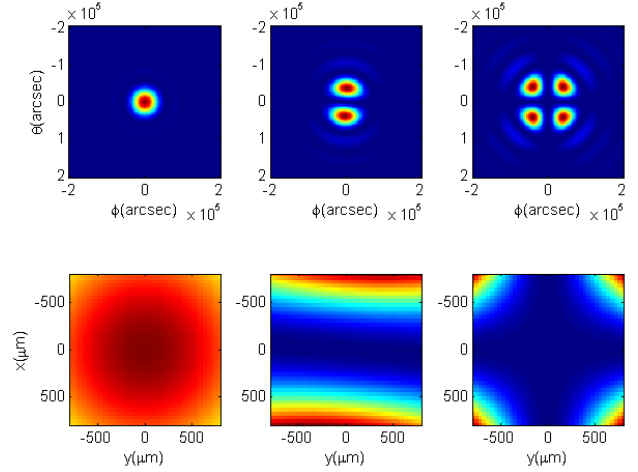


Fig. 2 Optical modes of the test system at $160 \mu\text{m}$

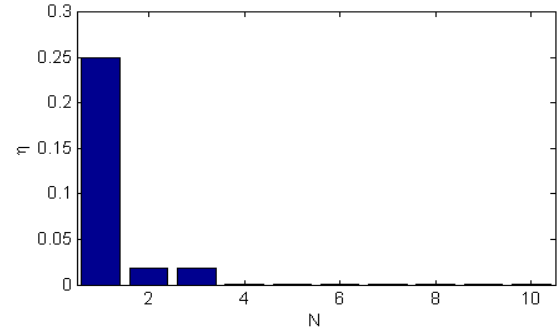


Fig. 3 Spectral throughputs of the 10 dominant optical modes over SAFARI L band at $160 \mu\text{m}$

B. Power Loading from Source

Fig. 4 shows the power loading of the source on the detector as a function of the temperature of the VTL for L-Band. The top curve corresponds to power arriving at the focal plane over the spatial footprint of a pixel, and the bottom curve corresponds to the total power incident on the absorber after having passed through the lightpipe. The ratio of the two is the coupling efficiency between the power in the optical modes and the power in the lightpipe modes.

C. Photon Noise from Source

Fig. 5 shows the noise power spectrum against frequency at 4 K for L-Band. The classical noise is extremely small compared with the photon noise, as would be expected at these wavelengths and temperatures. The noise power spectra at higher temperatures have also been calculated. It is found that classical noise is much smaller than photon noise across the all of the SAFARI wavebands, and therefore source-induced correlations between the outputs of two different pixels in an array can be neglected.

The total noise power can be calculated by integrating the noise power spectrum over the band. Fig. 6 shows the noise power level for L-Band as a function of temperature. The same procedures for calculating the noise levels were carried out in the case of the telescope's optical system to ensure that the two set of results are comparable.

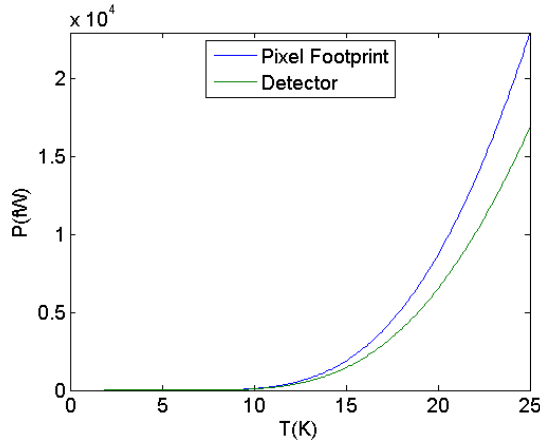


Fig. 4 Signal power in the L-Band as a function of source temperature

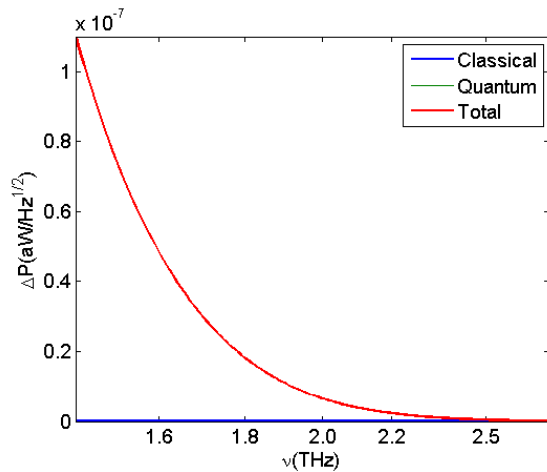


Fig. 5 Noise power spectra density across L-Band at 4 K

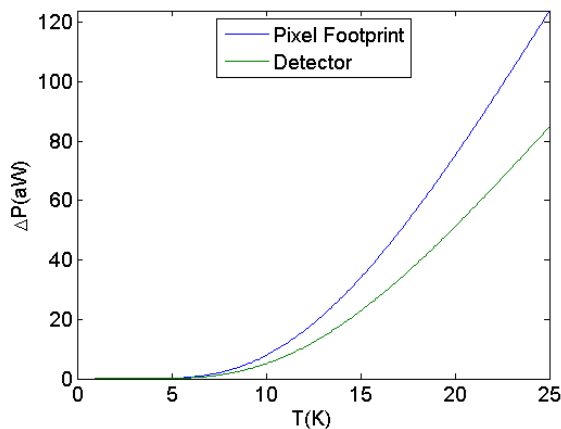


Fig. 6 Total noise power in L-Band from the blackbody source

The total noise power can be calculated by integrating the noise power spectrum over the band. Fig. 6 shows the noise power level for L-Band as a function of temperature. The

same procedures for calculating the noise levels were carried out in the case of the telescope's optical system to ensure that the two set of results are comparable.

D. Power Loading from Baffle

Fig. 7 shows the upper-limit baffle power level up to 4 K for L-Band. At 70 mK, the power loading from baffle is of order 10^{-18} fW, which is insignificant compared with the power loading from source. However, the power loading from the baffle increases rather rapidly with temperature, as a consequence of the upper frequency allowing for a large number of optical modes. Thus, it is crucial to keep the temperature of the baffle low.

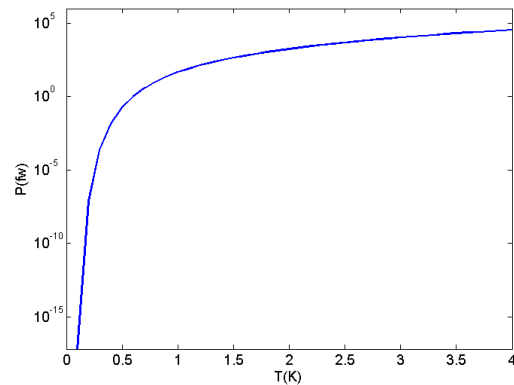


Fig. 7 Upper-limit power loading from baffle for L-Band

IV. CONCLUSIONS

We have developed an optical test system for ultra-low-noise Transition Edge Sensors. Crucially, we have, to our knowledge, for the first time established a theoretical and numerical model that is based on the natural optical modes of the test system, as distinct from the optical modes of the detector. We have shown that if the geometric focal ratio of the test system is that same as that of the equivalent optical system of the telescope, the optical modes and their individual throughputs are the same. This occurs even though the telescope has an effective thin lens whereas the test system does not. Thus the partially coherent illumination conditions are identical in both cases. We have also gone on to calculate the noise in the test system, and shown that based on photon noise alone the signal to noise ratio of our measurements will be high. Although we have described the technique in the context of SAFARI-like detectors, we believe that describing the behaviour of test systems in terms of modes will be valuable for many different instruments.

REFERENCES

- [1] P. D. Mauskopf, P. A. R. Ade, J. Beyer, M. Bruijn, J. R. Gao, D. Glowacka, D. Goldie, D. Giffin, N. J. Griffin, H. F. C. Howvers, P. Khosrapanah, P. Kooijma, P. A. J. De Korte, D. Morozov, A. Murphy, C. O'Sullivan, M. Ridder, N. Trappe, H. Van Weers, J. Van Der Kuur, S. Withington, "A TES focal plane for SPICA-SAFARI," ISSTT, pp. 246-255, Mar. 2010
- [2] E. D. Marquardt, J. P. Le, R. Radebaugh, "Cryogenic material properties database", 2000
- [3] G. Ventura, M. Barucci, E. Gottardi, I. Peroni, "Low temperature thermal conductivity of Kevlar", Cryogenics, vol. 40, pp.489-491, 2000

- [4] S. Withington, D. J. Goldie, C. N. Thomas (2013), "Partially Coherent Optical Modelling of the Ultra-Low-Noise Far-Infrared Imaging Arrays on the SPICA Mission", arxiv.org/abs/1307.7278
- [5] G. Saklatvala, S. Withington, M. P. Hobson, "Coupled-mode theory for infrared and submillimeter wave detectors", *J. Opt. Soc. Am. A*, Vol.24, 2006
- [6] S. Withington, G. Saklatvala, M. P. Hobson, "Theoretical analysis of astronomical phased arrays", *Journal of Optics*, 2008